

In utero exposure to diesel exhaust particulates is associated with an altered cardiac transcriptional response to transverse aortic constriction and altered DNA methylation

Jamie M. Goodson,* Chad S. Weldy,*[†] James W. MacDonald,[‡] Yonggang Liu,[†] Theo K. Bammler,[‡] Wei-Ming Chien,[†] and Michael T. Chin*^{†,1}

*Department of Pathology and [†]Division of Cardiology, Department of Medicine, University of Washington School of Medicine, and [‡]Department of Environmental and Occupational Health Sciences, University of Washington School of Public Health, University of Washington, Seattle, Washington, USA

ABSTRACT: *In utero* exposure to diesel exhaust air pollution has been associated with increased adult susceptibility to heart failure in mice, but the mechanisms by which this exposure promotes susceptibility to heart failure are poorly understood. To identify the potential transcriptional effects that mediate this susceptibility, we have performed RNA sequencing analysis on adult hearts from mice that were exposed to diesel exhaust *in utero* and that have subsequently undergone transverse aortic constriction. We identified 3 target genes, *Mir133a-2*, *Ptprf*, and *Pamr1*, which demonstrate dysregulation after exposure and aortic constriction. Examination of expression patterns in human heart tissues indicates a correlation between expression and heart failure. We subsequently assessed DNA methylation modifications at these candidate loci in neonatal cultured cardiac myocytes after *in utero* exposure to diesel exhaust and found that the promoter for *Mir133a-2* is differentially methylated. These target genes in the heart are the first genes to be identified that likely play an important role in mediating adult sensitivity to heart failure. We have also shown a change in DNA methylation within cardiomyocytes as a result of *in utero* exposure to diesel exhaust.—Goodson, J. M., Weldy, C. S., MacDonald, J. W., Liu, Y., Bammler, T. K., Chien, W.-M., Chin, M. T. *In utero* exposure to diesel exhaust particulates is associated with an altered cardiac transcriptional response to transverse aortic constriction and altered DNA methylation. FASEB J. 31, 4935–4945 (2017). www.fasebj.org

KEY WORDS: PM_{2.5} · heart failure · miR133a-2 · Ptprf · Pamr1

Exposure to particulate matter air pollution has been associated with respiratory (1, 2), cardiovascular (3–5), and cerebrovascular (6) disease. Exposure to fine particulate matter—particulate matter ≤ 2.5 μm (PM_{2.5})—has been linked to increased cardiovascular morbidity and mortality (3). Early life exposure to PM_{2.5} has been increasingly recognized for its impact on newborn health. Exposure to PM₁₀ during pregnancy has been linked with decreased birth weight, reduced placental weight (7), and placental oxidative and nitrosative stress (8), which further suggests that particulate matter air pollution contributes to placental insufficiency and intrauterine growth restriction.

ABBREVIATIONS: DE, diesel exhaust; FA, filtered air; FDR, false discovery rate; hmC, hydroxymethylcytosine; MBP, methyl-binding protein; NCBI, National Center for Biotechnology Information; PAH, polycyclic aromatic hydrocarbon; PM_{2.5}, particulate matter ≤ 2.5 μm ; TAC, transverse aortic constriction

¹ Correspondence: Center for Cardiovascular Biology, University of Washington School of Medicine, University of Washington, Brotman 353, Box 358050, 850 Republican St., Seattle, WA 98109, USA. E-mail: mtchin@u.washington.edu

doi: 10.1096/fj.201700032R

Placental insufficiency and intrauterine growth restriction has been implicated as an important determinant of adult cardiovascular health *via* the fetal origins of adult disease or Barker hypothesis pathway (9). These *in utero* PM exposures that induce placental insufficiency may predispose offspring to increased risk of disease, and, indeed, exposure to PM_{2.5} during the last trimester of pregnancy has been reported to be associated with increased newborn systolic blood pressure (10). Whereas prospective studies have not yet been carried out to determine whether the effects of maternal exposure affect the health of the offspring into adulthood, experimental studies that have used animal models raise the concern that *in utero* exposure to air pollution may be a strong determinant of adult health.

We have previously shown that *in utero* and early life exposure to diesel exhaust (DE) air pollution increases adult susceptibility to heart failure in mice, for which—after transverse aortic constriction (TAC) surgery—we observed decreased fractional shortening and increased left ventricular hypertrophy compared with filtered air (FA)—exposed control animals (11, 12). We have also reported that this increased adult susceptibility to heart

failure is conferred with *in utero* exposure only, which highlights the importance of the gestational window in mediating this long-lasting effect. Although we have identified placental vascular oxidative stress and inflammation as possible physiologic mechanisms, the molecular basis of increased heart failure susceptibility that persists from gestation to adulthood has not yet been elucidated.

One potential molecular mechanism with which to explain our observation of increased susceptibility to heart failure after *in utero* DE exposure involves epigenetic modification and altered transcription of key mediators. Air pollution has been demonstrated to alter DNA methylation both globally and at specific target genes. Human workplace exposure to PM₁₀ has been found to be associated with global hypomethylation at long interspersed nuclear element-1 and Alu repetitive DNA elements in circulating leukocytes, as well as decreased methylation at the iNOS promoter (13). A study of exposure to PM_{2.5} demonstrated a similar hypomethylation of DNA in peripheral blood leukocyte DNA (14). Exposure to PM_{2.5} during pregnancy has been associated with altered global DNA methylation profiles within placental tissue, where increased PM_{2.5} exposure was associated with lower global DNA methylation (15). This observation supports the hypothesis that developing fetal tissues *in utero* may be subject to particulate matter-induced alterations in DNA methylation. Altered DNA methylation in the developing myocardium as a result of exposure could persist into adulthood and influence the transcription of genes that are related to heart failure in our mouse model. To identify DE-responsive target genes that may be relevant to heart failure, we performed RNA sequencing of adult heart mRNA after *in utero* exposure to either DE or FA, followed by either TAC or sham surgery as adults, and have identified 3 potential target genes: *Mir133a-2*, *Ptprf*, and *Pamr1*. To determine whether alterations in DNA methylation play a role in the differential expression of these genes, we performed targeted bisulfite sequencing on CpG islands and promoters associated with these genes. We discuss the associated changes in DNA methylation and the potential role of these genes in mediating the increased susceptibility to heart failure that has been observed in this model.

MATERIALS AND METHODS

DE exposure and mice

C57BL/6 male and female mice were purchased from The Jackson Laboratory (Bar Harbor, ME, USA) and maintained as an inbred line. All mice were housed in specific pathogen-free conditions on a 12-h light/dark cycle. Female and male mice between ages of 12 and 14 wk were transferred to our Northlake Diesel Exposure Facility located near the University of Washington and housed under specific pathogen-free conditions in Allentown caging systems (Allentown, NJ, USA) as previously described (11, 12, 16–19). All animal experiments were approved by the University of Washington Institutional Animal Care and Use Committee (4134-01). DE was generated from a single cylinder Yanmar diesel engine (Model YDG5500EV-6EI; Osaka, Japan) operating on 82% load. A detailed analysis of DE particulate components in this system has been previously reported

(17). DE exposures were conducted for 6 h/d (9 AM–3 PM) 5 d/wk (Monday–Friday), and DE concentrations were regulated to ~300 µg/m³ of PM_{2.5}. A 300-µg/m³ concentration of PM_{2.5} 6 h/d, 5 d/wk equates to a time-weighted hourly average of 53 µg/m³. Exposure characteristics that detailed gas, particle-bound polycyclic aromatic hydrocarbons (PAHs), and particle diameter were recently measured and reported (11, 19).

Female mice were paired with males for timed mating in FA. After observation of a vaginal plug, pregnant mice were put into FA or DE, with exposures beginning at embryonic day (E)0.5 and lasting until E17.5. Neonates were used for neonatal cardiomyocyte preparation (described below) or were saved for adult surgery. Offspring were raised in FA until 11 wk, at which time they underwent baseline echocardiography and TAC at 12 wk using a 27-gauge needle. Serial echocardiographic measurement, gravimetry, and histology for these mice have been previously published (12). Hearts from these mice were harvested at 15 wk, rapidly frozen in liquid nitrogen, and stored at –80°C before RNA isolation. The *in utero* exposure and sample collection scheme is displayed in Fig. 1.

RNA isolation, sequencing, and bioinformatics analysis

RNA was isolated from fresh-frozen hearts of 3 mice per group by using an miRNeasy Kit (Qiagen, Germantown, MD, USA) according to manufacturer protocol. RNA sequencing was performed using the Ion Torrent Proton (Thermo Fisher Scientific, Waltham, MA, USA). In brief, RNA samples were depleted of ribosomal RNA by using the Low Input RiboMinus Eukaryotic System kit (v.2; Thermo Fisher Scientific). cDNA library was then created with the ribosomal-depleted RNA by using the Ion Total RNA sequencing kit (v.2; Thermo Fisher Scientific). This included fragmentation *via* RNase III, hybridizing and ligating the RNA, performing reverse transcription, and amplification. Samples were labeled with the Ion Xpress RNA sequencing barcode 1–16 kit (Thermo Fisher Scientific) to enable the multiplexing of 4 samples per run. Templating, loading, and sequencing were carried out by using the Ion PI Template OT2 200 Kit (v.2), the Ion PI Chip Kit (v.2), and the Ion PI Sequencing 200 Kit (v.2), respectively (all from Thermo Fisher Scientific). Data were generated by using the included Ion Reporter software (Thermo Fisher Scientific). Sequences were aligned to the mm10 mouse genome by using the subread aligner (20), and counts were generated by using the Bioconductor Rsubread package (University of California, Santa Cruz, CA, USA). Comparisons were performed by using the Bioconductor edgeR package (Roswell Park Cancer Institute, Buffalo, NY, USA; bioconductor.org). Genes were identified as significantly different between groups if they had both a false discovery rate (FDR)-adjusted value of $P \leq 0.05$ and an absolute fold change of ≥ 1.5 . The full data set has been deposited in the National Center for Biotechnology Information (NCBI) GEO Database (Accession No. GSE91398; Bethesda, MD, USA: <https://www.ncbi.nlm.nih.gov/genbank/>).

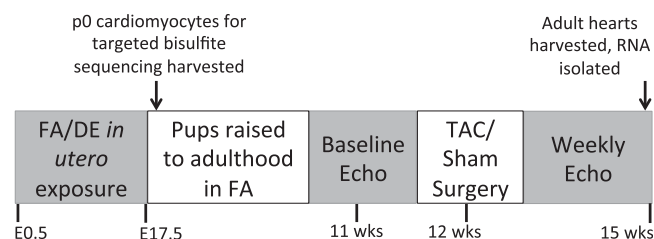


Figure 1. Exposure and sample collection scheme.

Quantitative RT-PCR analysis

cDNA was synthesized with the iScript Reverse Transcription Supermix kit (Bio-Rad, Hercules, CA, USA) using RNA from 4 FA sham-treated, 7 FA TAC, 4 DE sham-treated, and 6 DE TAC hearts, each group including the 3 samples used in RNA sequencing, and differential gene expression was validated by quantitative RT-PCR using the iTaq Universal Sybr Green Supermix (Bio-Rad). The following primers were used for validation: miR133a-2: (forward) 5'-GCCAAATGCTTTGCT-GAAGCTG-3', (reverse) 5'-GCTGGTTGAAGGGGACCAAA-3'; Ptpf: (forward) 5'-CAACGATGGGCTCAAGTCT-3', (reverse) 5'-TTCTTGGGCTTGTTACCTC-3'; Pamr1: (forward) 5'-CCCAGGAAAGAAGGAAGTGG-3', (reverse) 5'-GGCAGCT-CTTGACATTTTCA-3'; and 18S: (forward) 5'-GGACAGGA-TTGACAGATTGATAG-3', (reverse) 5'-ATCGCTCCACCAAC-TAAGAA-3'. Samples were cycled at 95°C for 15 s, 60°C for 1 min for 40 cycles. Samples were run on the 7900HT Fast Real-Time PCR System (Applied Biosystems, Foster City, CA, USA). Expression of Ptpf, miR133a-2, and Pamr1 was normalized to ribosomal RNA 18S. Statistical analysis was carried out by using 2-way ANOVA for comparison of expression values and with linear regression for comparison of expression value to ventricle weight.

Assessment of candidate gene expression in human heart failure samples

To determine whether the identified candidate genes demonstrated differential expression in human heart failure, we examined their expression patterns in a published human nondiabetic heart failure and control myocardial biopsy data set (21) that is available *via* the NCBI GEO database (Accession No. GSE26887). Statistically significant differences in gene expression were determined by using 1-way ANOVA with Bonferroni correction.

Isolation of neonatal cardiomyocytes

Upon birth, neonatal hearts were harvested, trimmed of surrounding vascular and atrial tissue, and dissociated as previously described (22, 23). Dissociation was performed by using 1 mg/ml Liberase TH (Roche, Pleasanton, CA, USA) in 1× HBSS by

incubating hearts at 37°C for 5 min in solution, with pipetting to release cells after incubation. Medium that contained released neonatal cardiomyocytes was adjusted to 20% FBS-DMEM, and cellular dissociation was continued until the majority of cells were released. Cells were then filtered by using a 70- μ m sieve, re-eluted in 20% FBS-DMEM with 20 μ m Ara-C, and incubated at 37° for 1 h to allow fibroblasts to attach to the plate. After incubation, media with suspended cardiomyocytes was carefully removed and spun, and purified cardiomyocyte pellets were collected and frozen at -80°C.

DNA isolation and targeted bisulfite sequencing

DNA was isolated from purified neonatal cardiomyocytes of 8 DE- and 6 FA-exposed p0 mice by using the DNeasy Blood and Tissue Kit (Qiagen) according to the manufacturer's protocol. DNA was bisulfite-converted by using EpiTect Fast Bisulfite Conversion kit (Qiagen) according to the manufacturer's protocol. Converted DNA was amplified by using HotStarTaq Master Mix (Qiagen), activated at 95°C for 15 min, cycled at 94°C for 30 s, 63°C for 45 s (-1°C/cycle for the first 10 cycles), 68°C for 1 min for 10 cycles, for 40 cycles. The following primers were used, targeting the regions boxed in red shown in Fig. 2:

GM6307 promoter: (forward) 5'-GTATTGGGTTTTGTTAA-AAATAGTAGG-3', (reverse) 3'-CCTCACCTTAATAATTCTT-ATATACCC-5'; GM6307 exon 1.1: (forward) 5'-GGGTATA-TAAGAATTATTAAGGTGAGG-3', (reverse) 5'-CAAACC-CAACTACACACCTTAC-3'; GM6307 exon 1.2: (forward) 5'-GTAGGAGGGTTGGGGGAA-3', reverse: 5'-CAACCAACTA-AAAAAAECTCACC-3'; Ptpf CpG17: (forward) 5'-GTAT-TTGGTTTGTAGTTTTTGGATGTG-3', (reverse) 5'-CAAACCT-ACTTCTCCTCAATAC-3'; Ptpf CpG24: (forward) 5'-TTTTTAGGTGTTGTAAGGAAGTTAAT-3', (reverse) 5'-TACACTATTCTAAACCCTAACAAAC-3'; Ptpf CpG79.1: (forward) 5'-ATTGGAAGGGAGAGAAATTA-3', (reverse) 5'-CCCCRTACAAAATTTCCC-3'; Ptpf CpG79.2: (forward) 5'-GGGAAATTTGTAYGGGGG-3', (reverse) 5'-CCTACAA-CTCCACTCTCTACAAAC-3'; Pamr1 promoter: (forward) 5'-GGTTTTAGTTAGTGTGTTTGTATA-3', (reverse) 5'-AAC-TCTCCACCCTCAACTAAAA-3'; and Pamr1 exon 1: (forward) 5'-TTTTAGTTGAGGGTGGGAGAGTT-3', (reverse) 5'-CAAAA-AACTCCTAATCACTAACAAATAC-3'.

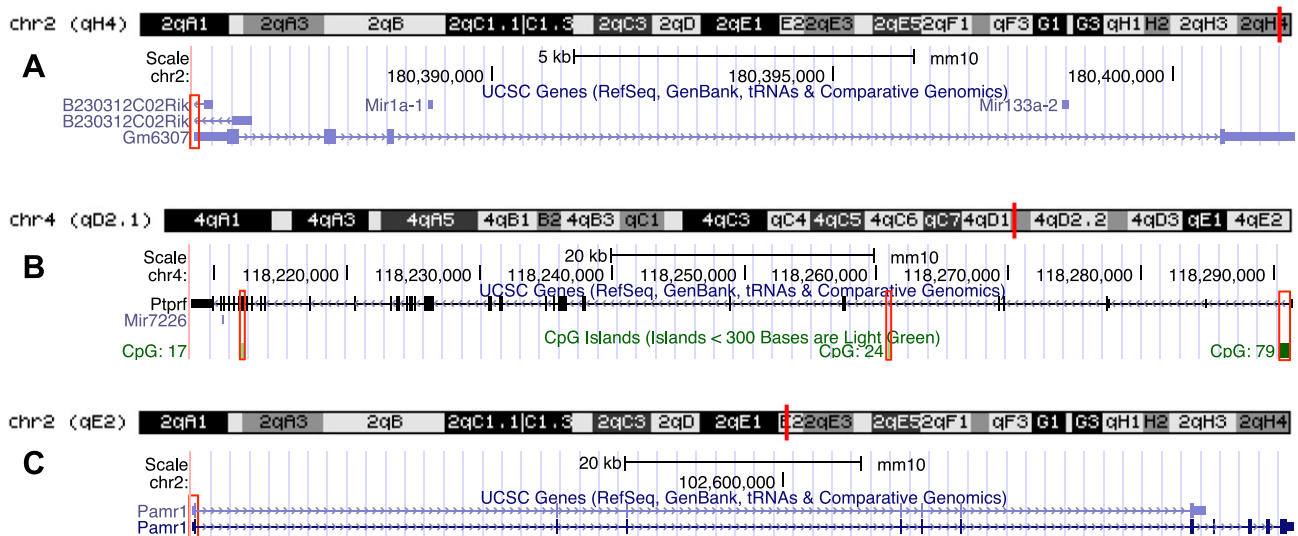


Figure 2. Genomic regions for bisulfite sequencing. Genomic regions highlighted in red boxes are areas that were targeted for bisulfite sequencing. Targets correspond to GM6307 promoter and first exon (A); Ptpf CpG islands 17, 24, and 79 (B); and Pamr1 promoter and first exon (C).

Bisulfite-converted DNA was sequenced in the University of Washington Northwest Genomics Center by using an Illumina MiSeq (Illumina, San Diego, CA, USA) in paired-end mode, 250-bp read length. Samples were sequenced to a mean depth of approximately 0.5 million reads. Adapter sequences and low-quality bases were removed from the raw reads by using Trimmomatic (v.0.32) (24). In brief, we removed Illumina TruSeq3 adaptors, then excluded any bases on either end of the read with a quality score <3, then used a moving window approach to trim off any portion of the read in which the average quality score over a 4-base moving window dropped <15. Any reads that were <36 bp in length after trimming were excluded. We then aligned trimmed reads against the mouse mm10 genome by using the Bismark aligner (v.0.15.0) (25) in conjunction with the bowtie aligner (v.0.12.8) (26). The trimming process resulted in a set of reads that remained paired as well as sets of reads that were unpaired—because the matching pair is missing or was excluded. We aligned the paired and unpaired reads separately, then combined the resulting BAM files before extracting methylation calls by using Bismark's methylation_extractor function.

We read the per-base methylation calls from Bismark into R by using the Bioconductor bsseq package (27). To minimize low-quality methylation calls, we excluded any CpG with a read coverage of <5 in more than one half of samples. Individual CpG methylation estimates are known to be highly variable, so we smoothed the methylation estimates over adjacent bases by computing a moving average of all CpG sites within a 100-base moving window. We then made comparisons between groups at each CpG site by using the Bioconductor DSS package (28). In brief, we modeled the smoothed methylation estimates (at each CpG) on the basis of the β -binomial distribution, estimating the dispersion parameter by using a bayesian hierarchical model. We then computed a Wald statistic for each CpG site. Our goal was to find genomic regions that seem to be consistently differentially methylated between DE- and FA-exposed mice. We defined a differentially methylated genomic region on the basis of several criteria: the region had to be at least 50 bp long and contain at least 3 CpGs, and at least 50% of the CpGs had to have a Wald value of $P < 0.01$.

RESULTS

Transcriptional profiling by RNA sequencing reveals candidate target genes in the heart induced by *in utero* DE exposure

Table 1 shows the various comparison groups, the number of candidates that were identified by unadjusted values of $P < 0.05$, and those that were identified after multiple hypothesis correction controlling for FDR. The number of genes that were differentially expressed (FDR < 0.05 and absolute fold change > 1.5) after TAC was 880 in DE-exposed groups and 432 in FA-exposed groups. In contrast, the number of genes that were differentially expressed after DE exposure was 5 in the sham-treated group and 2 in the TAC group. These findings indicate that the magnitude of the TAC effect is much greater than that of the DE effect. Because gene expression after TAC has been studied extensively, we have focused primarily on genes that were affected by DE and do not discuss genes induced by TAC any further.

Table 2 shows the 5 genes that were differentially expressed in DE and FA groups after sham surgery. Three of these genes, *Gm8841*, *Pcdh1*, and *Bbip1*, demonstrate a

TABLE 1. Number of genes that were altered in expression as a result of exposure, surgery type, or interaction

Comparison	Unadjusted $P < 0.05$	FDR < 0.05
DE TAC vs. DE sham	1375	880
DE sham vs. FA sham	316	5
DE TAC vs. FA TAC	153	2
FA TAC vs. FA sham	931	432
Interaction	321	3

reduction in expression after DE exposure, whereas the remaining 2 genes, *Mir133a-2* and *Gck*, show increased expression. Table 3 shows the 2 genes that were differentially expressed in DE and FA groups after TAC surgery. *Ptprf* demonstrates increased expression, whereas *Pdk4* shows reduced expression. Table 4 lists genes that were identified in the interaction comparison, which identifies genes that respond differently to TAC, depending on exposure. These genes included *Ptprf*, *Mir133a-2*, and *Pamr1*.

Additional validation of individual candidate gene expression from the interaction group by quantitative RT-PCR revealed interesting patterns of gene expression. On the basis of their statistically significant differences in expression across all 4 surgery and exposure conditions, we concluded that these candidates are likely to be important in the mediation of DE-induced susceptibility to heart failure. Expression of *mir133a-2* demonstrated divergent regulation in adult hearts after exposure to DE *in utero*. DE-exposed mice that underwent sham surgery had elevated expression compared with FA controls, but TAC surgery induced a marked suppression of expression, whereas FA-exposed animals showed an induction of expression (Fig. 3A). Reduced expression of *mir133a-2* after TAC is associated with worse heart failure and fibrosis. These findings are consistent with the previously reported role of miR133a-2 in functioning to suppress pathologic cardiac hypertrophy and fibrosis (29, 30).

Expression of *Ptprf*, which encodes the protein, tyrosine phosphatase, receptor type, F (also known as leukocyte common antigen-related phosphatase), was not significantly changed by DE in mice that underwent sham surgery. In mice that underwent TAC, those that were exposed to DE *in utero* showed an increase in expression compared with those that were exposed to FA (Fig. 3C). This elevated expression is associated with worse heart failure and cardiac fibrosis, and is consistent with a causal role for PTPRF in promoting pathologic hypertrophy and heart failure.

TABLE 2. Top 5 specific genes induced by DE in sham-treated animals (i.e., DE sham-treated vs. FA sham-treated)

Gene symbol	LogFC	P	FDR
<i>Gm8841</i>	-1.140	3.33e-08	0.000344
<i>Pcdh1</i>	-0.895	6.97e-07	0.002490
<i>Bbip1</i>	-1.130	7.24e-07	0.002490
<i>Mir133a-2</i>	1.970	1.21e-05	0.027200
<i>Gck</i>	1.180	1.32e-05	0.027200

TABLE 3. *Specific genes induced by DE in TAC-treated animals (i.e., DE TAC vs. FA TAC)*

Gene	LogFC	P	FDR
<i>Ptprf</i>	1.580	6.09e-08	0.000628
<i>Pdk4</i>	-1.100	1.25e-06	0.006440

FDR, false discovery rate.

Expression of *Pamr1*, which encodes peptidase domain-containing associated with muscle regeneration 1, was also increased as a result of exposure. *Pamr1* expression is increased in both FA- and DE-exposed mice after TAC, although the increase is larger in the DE cohort. Expression of *Pamr1* also demonstrated a significant correlation with the ventricular weight-to-tibia length ratio (Fig. 3E). This elevated *Pamr1* expression, like that of *Ptprf*, is associated with worse heart failure and cardiac fibrosis, and is also consistent with a causal role for *Pamr1* in the promotion of pathologic hypertrophy and heart failure.

***Ptprf*, *miR133a-2*, and *Pamr1* gene expression are altered in a human heart failure gene expression data set**

To determine whether the identified target genes demonstrated altered expression in human heart failure, we examined their expression in a publicly available Affymetrix data set (NCBI, Accession No. GSE26887) that was derived from human myocardial biopsies that were taken from patients with nondiabetic heart failure or control hearts (21). *Mir133a* expression is reduced in both forms of heart failure, which is consistent with a role in protecting against heart failure; however, examination of *Ptprf* and *Pamr1* expression indicates that both genes show significant increases in expression in nondiabetic heart failure compared with controls (Fig. 4). These expression patterns are consistent with a role for these genes in contributing to human heart failure.

DNA methylation patterns at the *Ptprf*, *Pamr1*, and *miR133a-2* loci

In our model of DE-related heart failure, exposure to DE occurred only during gestation, with no exposure after birth, yet these mice developed significantly worsened heart failure as adults after TAC. This suggests that long-lasting epigenetic modifications, such as DNA methylation, are responsible for this susceptibility. To test this, we

TABLE 4. *Specific genes showing a differential response to TAC, depending on exposure (i.e., interaction)*

Gene	logFC	P	FDR
<i>Ptprf</i>	-2.380	2.29e-08	0.000236
<i>Mir133a-2</i>	3.120	6.64e-07	0.003430
<i>Pamr1</i>	-2.630	4.03e-06	0.013900

performed targeted bisulfite sequencing at CpG islands and promoter regions that were associated with *Ptprf*, *miR133a-2*, and *Pamr1* from neonatal cardiomyocytes of mice that were exposed to FA or DE *in utero*. We found that whereas *in utero* DE exposure did not induce significant differences in DNA methylation in either the *Pamr1* or *Ptprf* loci (data not shown), the first exon of GM6307—the gene in which *miR133a-2* resides—had decreased methylation on the basis of the criteria discussed above and in the legend for Fig. 5. This finding is consistent with the elevated expression of *miR133a-2* in hearts from mice that were exposed to DE in the sham-surgery group (Fig. 3A).

DISCUSSION

We have demonstrated that gene transcription is significantly altered in mice as result of *in utero* DE exposure and adult TAC surgery. We identified the genes *Ptprf*, *miR133a-2*, and *Pamr1* as being differentially regulated and verified these findings by quantitative RT-PCR. To the best of our knowledge, these genes have not been previously identified as being responsive to DE exposure in the heart. Whereas the exposure level used in this study (300 $\mu\text{g}/\text{m}^3$) is well above the 2015 national average for the United States (8 $\mu\text{g}/\text{m}^3$), such countries as Egypt and Saudi Arabia have averages of approximately 100 $\mu\text{g}/\text{m}^3$ (31), and in 2013, Beijing reached a record of almost 1000 $\mu\text{g}/\text{m}^3$. In addition, occupational exposure is of great concern. One study demonstrated that workers in high-exposure settings, such as tunnel construction, can receive exposures of up to 400 $\mu\text{g}/\text{m}^3$ PM_{2.5} (32), and those who work in steel plants can reach exposure levels >1200 $\mu\text{g}/\text{m}^3$ PM₁₀ (13). Our exposure levels in this study thus reflect real-world human exposure.

It has been postulated that PAMR1 plays a role in the regeneration of skeletal muscle on the basis of its expression pattern (33), to play a role in the acute insulin response to glucose (34), and to be suppressed by promoter methylation in breast cancer (35). To the best of our knowledge, no functional studies have been published, and a role for PAMR1 in cardiac hypertrophy and heart failure has not been reported. It is unclear whether these changes in gene expression have individual roles in the development of DE-induced heart failure, or if the combination of these gene changes is required. The expression pattern indicates that increased expression is associated with increased cardiac hypertrophy and fibrosis.

PTPRF and other tyrosine phosphatases play critical roles in the mediation of signal transduction by limiting intracellular phosphorylation cascades that occur after autophosphorylation of receptor tyrosine kinases (36, 37). Overexpression of *Ptprf* has been shown to limit insulin sensitivity and, thus, promote insulin resistance in mouse models, whereas knockdown enhances insulin sensitivity in cultured cells (38–40). Common single-nucleotide polymorphisms in *Ptprf* are associated with the development of coronary artery disease in patients with type 2 diabetes (41). Previous work using *in vitro* models has shown that *Ptprf* expression is decreased after treatment with TNF- α , and that *Ptprf* expression is readily modified

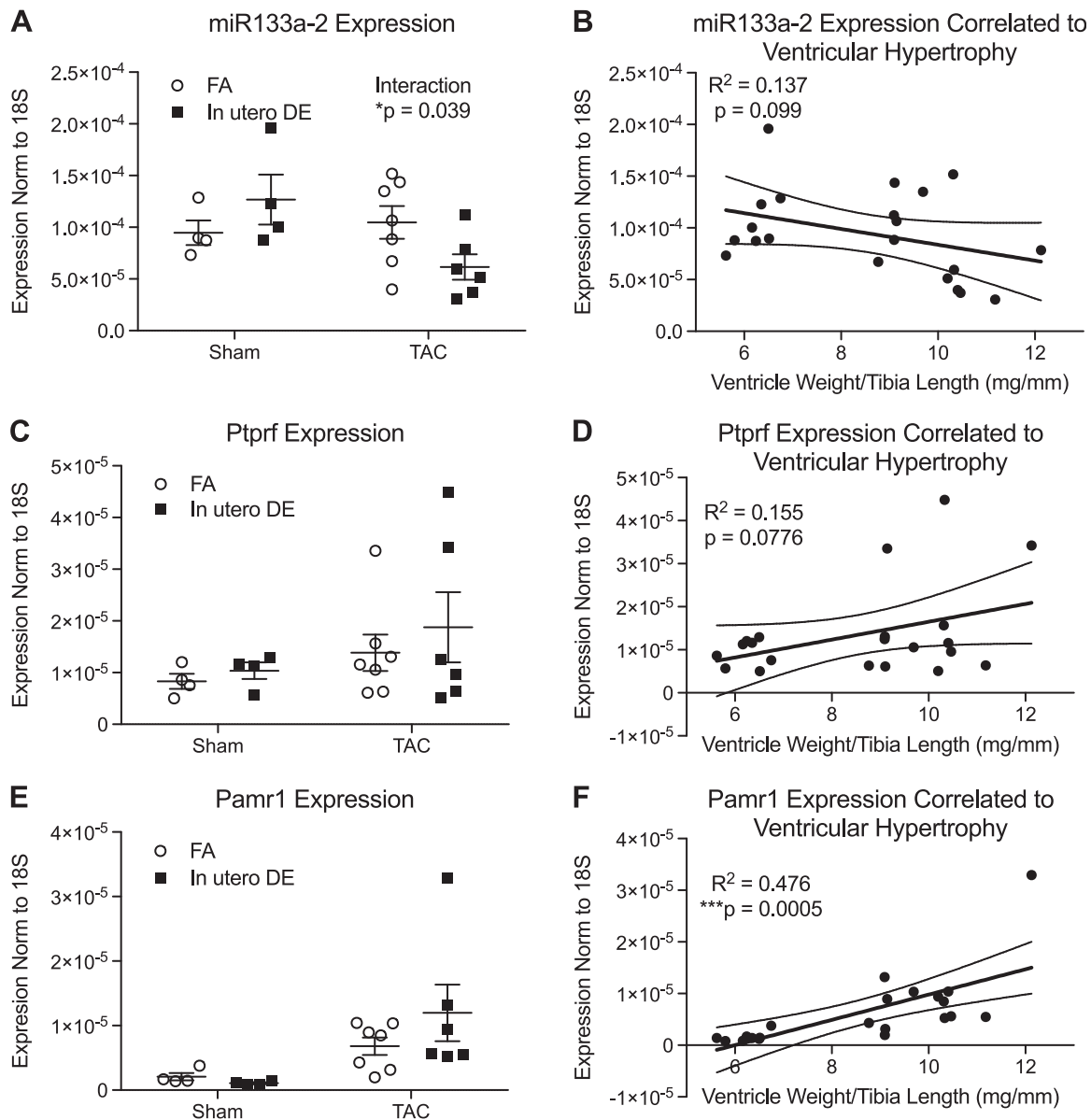


Figure 3. Expression of miR133a-2, PTPRF, and Pamr1 after *in utero* DE exposure and TAC surgery, correlated with ventricular weight/tibia length measurements. *A, C, E*) $\Delta\Delta C_t$ values for miR133a-2 (*A*), Ptpfr (*C*), and Pamr1 (*E*) in the 4 categories: FA sham-treated, DE sham-treated, FA TAC, and DE TAC. *B, D, F*) Corresponding linear regression values for miR133a-2 (*B*), Ptpfr (*D*), and Pamr1 (*F*), plotting expression as a function of ventricle weight normalized to tibia length. * $P < 0.05$.

to regulate cell signaling (42). To the best of our knowledge, PTPRF has not previously been associated with the development of heart failure. On the basis of its expression pattern, we hypothesize that exaggerated expression in hearts after *in utero* DE exposure likely either potentiates pathologic hypertrophic signaling or limits antihypertrophic signaling.

A role for miR133a in cardiac hypertrophy is better established. *miR133a-2* encodes a premature form of miR133a, which controls cardiac development (43). Reduced expression of miR133a leads to the enhancement of cardiac hypertrophy *in vitro* by increased expression of its target, inositol 1,4,5-trisphosphate type II (44). Overexpression of miR133a in the heart has been reported to suppress cardiac fibrosis, but not cardiac hypertrophy, after TAC (30), which is consistent with our results.

MiR133a loss of function has previously been associated with myocyte apoptosis after ischemia-reperfusion *via* increased expression of caspase 9 (45) and skeletal muscle myopathy *via* an effect on its target, dynamin 2 (46). DNA hypermethylation of a CpG island that was associated with the miR133a-2 cluster and reduced *miR133a-2* expression have been associated with colorectal cancer (47). In comparison, our results demonstrate that *in utero* DE resulted in a ~2-fold increase in *miR133a-2* expression at baseline in our sham-treated mice (Fig. 3*A* and Table 2). Our previously reported baseline phenotypic assessment in sham-treated mice did not reveal *in utero* DE exposure to have any effect on cardiac function or myocyte hypertrophy (12). We observed this increased *miR133a-2* expression to be down-regulated after TAC in *in utero* DE-exposed mice (Fig. 3*A* and Table 1), with a simultaneous increase in

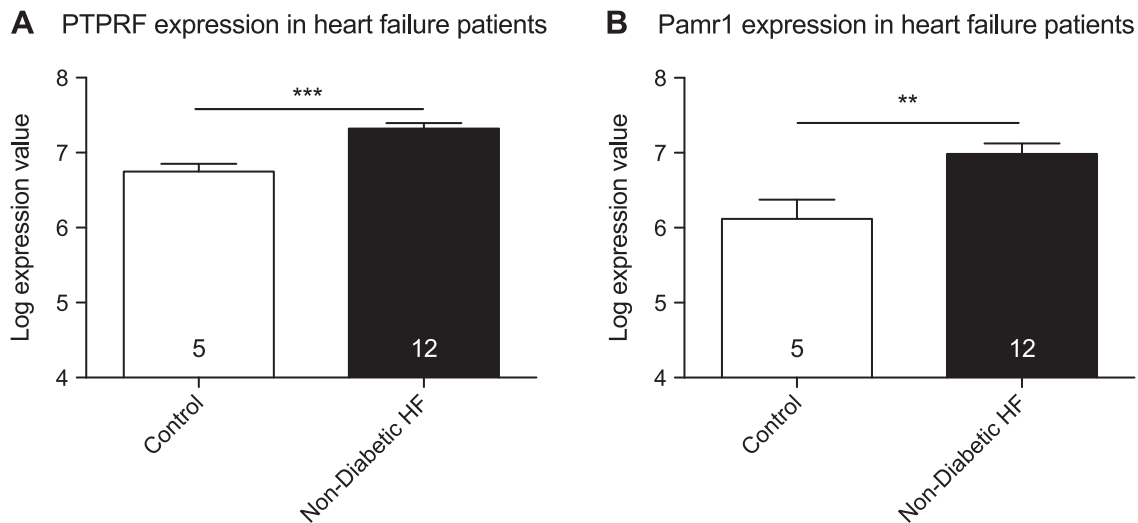


Figure 4. Expression of *Ptprf* (A) and *Pamr1* (B) in human heart failure samples. Significance was calculated by using 1-way ANOVA with *post hoc* Bonferroni. Data were derived from publicly available Affymetrix data set (NCBI GEO Accession No. GSE26887). ** $P < 0.005$, *** $P < 0.0005$.

left ventricle wall thickness, fibrosis, and decreased fractional shortening, as previously reported (12). This down-regulation of *miR133a-2* with concomitant exacerbation of heart failure with reduced ejection fraction may suggest that the increased *miR133a-2* expression at baseline played a protective role in preserving cardiac function, and that loss of this increased expression results in the exacerbation of heart failure. Our DNA methylation studies in neonatal cardiomyocytes reveal hypomethylation within the first exon of *GM6307*, which is consistent with our observation of increased *miR133a-2* expression in baseline sham-treated mice. The loss of increased *miR133a-2* expression in *in utero* DE-exposed mice in heart failure implies that there may be dynamic modifications of DNA methylation or multifactorial changes in chromatin assembly and transcription factor accessibility modified by *in utero* DE exposure. These observations suggest that baseline hypomethylation and increased *miR133a-2* expression at baseline are advantageous adaptations, but that the dysregulation of its expression in heart failure is uniquely affected by *in utero* DE exposure. Loss of *miR133a-2* overexpression in DE-treated hearts after TAC may facilitate pathologic hypertrophy by enhanced IP(3)RII signaling and increased apoptosis mediated by caspase 9 (44).

The effect of environmental toxicant exposure on cardiac hypertrophy *via* regulation of *miR133a* expression and DNA methylation has been previously reported (48). Exposure to the PAH, phenanthrene, causes cardiac and myocyte hypertrophy in both *in vivo* and *in vitro* models. In male Sprague-Dawley rats and the H9C2 rat cardiomyoblast cell line, phenanthrene exposure was associated with a decrease in *miR133a* expression and a simultaneous increase in protein levels of important *miR133a* cardiac hypertrophy targets, *Cdc42* and *RhoA*. This decrease in *miR133a* expression was associated with an increase in DNA methylation at 5 CpG sites that were located near the putative transcription start site of *miR133a* in H9C2 cells. Overexpression of *miR133a* *via* transfection of *miR133a* mimetics, or inhibition of DNA methylation with a DNA

methylation inhibitor (5-aza-2'-deoxycytidine), largely eliminated the hypertrophic effect of phenanthrene. PAHs are a significant component of DE particulate mass, and we have previously reported our DE exposure system to generate DE with a mass fraction of particle-bound PAH at 20 ng/ μ g (11). Phenanthrene is a major constituent of environmental PAHs and has been reported to be a significant component of DE (49), which suggests that PAHs, including phenanthrene, may possibly contribute to our observed effects on heart failure and DNA methylation. Although we observed *in utero* DE exposure to result in altered *miR133a-2* expression in a manner that was similar to that reported previously (48), our observed DNA methylation results of hypomethylation of the first exon are in contrast and perhaps suggests a unique epigenetic mechanism of action in *in utero* DE-induced adult susceptibility to heart failure.

One surprising finding of our work is that relatively few genes are significantly affected in the heart after *in utero* DE exposure, but we believe that this finding is likely a result of dilutional effects from using whole-heart RNA. Future studies using adult cardiomyocyte RNA sequencing would likely generate additional candidate genes. Another unaddressed question is the effect of *in utero* DE exposure on the global DNA methylation pattern in cardiomyocytes. We have attempted to perform genome-wide bisulfite sequencing in whole adult heart DNA, but to date no differentially methylated regions have been consistently identified, likely because of the dilutional effect of noncardiomyocytes. Previous studies of methylation in adult cardiomyocytes have relied on the purification of adult cardiomyocytes (50). A future study that analyzes DNA methylation patterns in isolated adult cardiomyocytes will address this question.

Another potential caveat of studying whole-heart RNA is that gene expression changes may reflect a shift in cell population rather than a change in expression within a given cell type. We do not favor this hypothesis, as both *miR133a-2* and *Pamr1* are expressed predominantly in

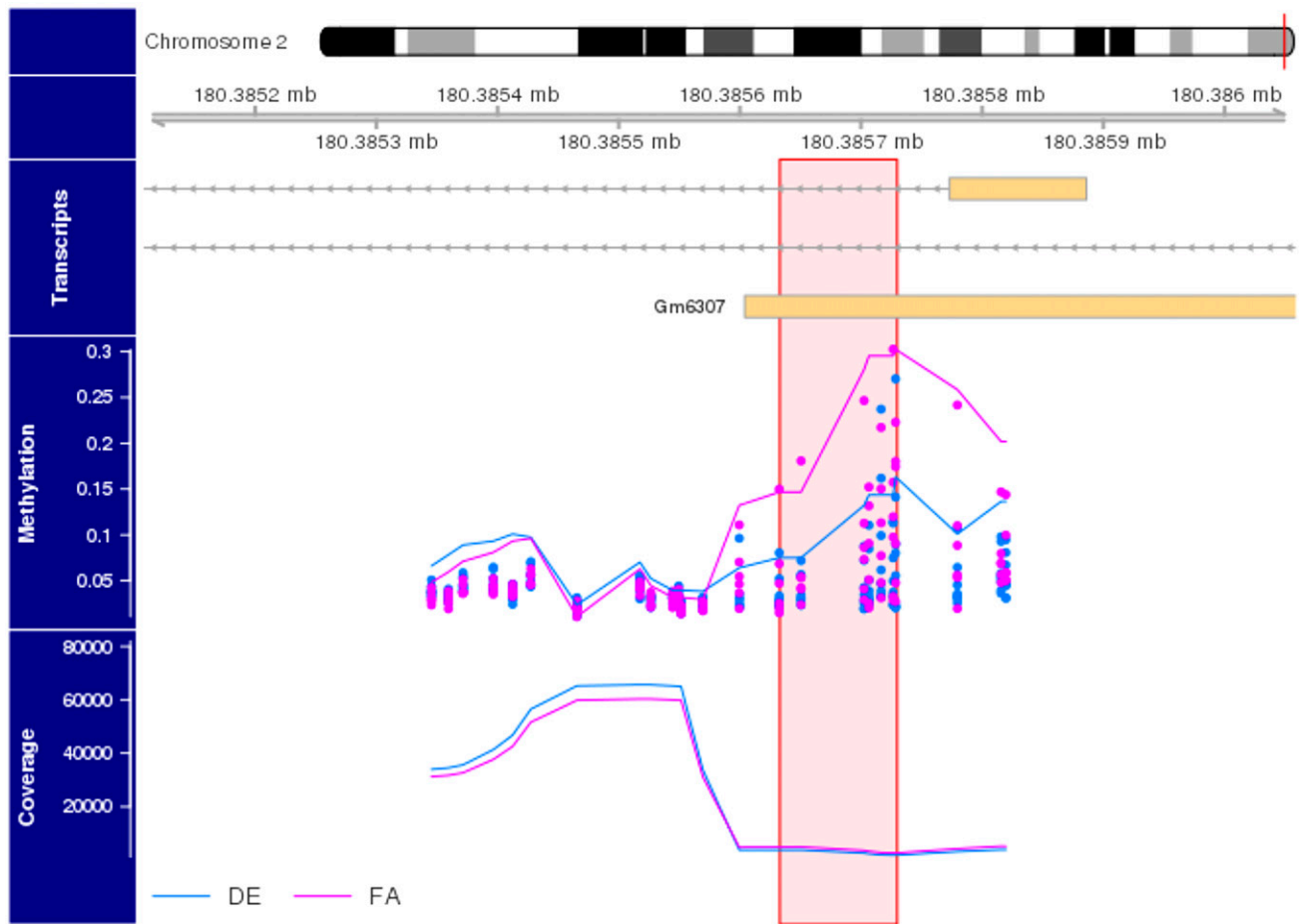


Figure 5. Targeted bisulfite sequencing of GM6307 promoter and exon 1. The upper portion of the plot contains a karyogram of chromosome 2, with a vertical red bar showing the region of interest; the horizontal bar just below the karyogram shows the zoomed-in region of the chromosome being inspected. The transcripts portion of the plot presents University of California, Santa Cruz (UCSC) genome browser-style transcripts, where the orange bars represent exons and the gray lines represent introns. Arrows in the intronic region represent the direction of transcription. Below that, we present the observed (individual points) and smoothed (lines) percent methylation estimates for CpGs in this genomic region. Pink points and lines represent FA samples, whereas blue represent DE samples. In the lowest (coverage) portion of the plot we present the sequencing read depth (e.g., the number of sequencing reads that aligned over each CpG). The pink vertical bar indicates the genomic region that seems to be differentially methylated. This region spans 96 bp and contains 7 CpGs, all of which indicate a decrease in methylation in DE-exposed animals at a Wald value of $P < 0.01$.

muscle tissue (30, 33), and the relative contribution of additional cells, such as inflammatory cells, is still likely to be modest compared with cardiomyocytes and fibroblasts.

Although it has been demonstrated in multiple studies that exposure to PM_{2.5} is associated with changes in DNA methylation (13–15), the mechanism is unclear. In our study, we initially assessed whether the DNA methylases, DNMT1, DNMT2, or DNMT3, were differentially expressed by using quantitative RT-PCR, but did not observe any significant difference, which is consistent with our RNA sequencing data (data not shown). It has been shown that exposure to DE increases reactive oxygen species production (51, 52), which, in turn, can interact with DNA to oxidize methylcytosine to hydroxymethylcytosine (hmC). hmC has been shown to prevent methyl-binding proteins (MBPs) from binding to methylated cytosines (53). This can prevent the normal chromatin silencing that would occur at these sites, which allows for transcriptional expression. Furthermore,

oxidation to hmC has been shown itself to be an intermediary to the potential loss of DNA methylation (54, 55). In addition to the role of hmC as both a blockade of chromatin silencing and a stepping stone to loss of methylation, the guanine oxidative lesion, 8-oxoguanine, also can inhibit the binding of MBPs, which prevents the silencing of chromatin regions (53). Taken together, these processes could explain the observation of changes in DNA methylation associated with exposure to DE.

The findings of decreased DNA methylation at the first exon of GM6307 are intriguing, as it gives credence to the idea that *in utero* exposure to DE affects the developing heart *via* altered epigenetic patterning. DNA methylation of the first exon has been shown to control gene regulation (56), and decreased DNA methylation in DE-exposed mice correlates with the higher expression observed in adults that have undergone sham surgery. However, the DE-exposed, TAC surgery group demonstrated a reduction in expression, which is not explained by our DNA

methylation findings and perhaps is because of other epigenetic modifications or altered signaling as a result of the surgery.

A limitation of our work is that the changes in gene expression represent associations and do not demonstrate causality. Our initial attempts to investigate effects of *in utero* DE exposure on TAC-induced heart failure in mice that overexpress *miR133a* in the heart were inconclusive because the wild-type FVB strain that has been used to generate these mice is not susceptible to TAC-induced heart failure after *in utero* DE exposure (data not shown), in contrast to the C57BL/6 strain that was used in this study and previously reported studies (12). We also isolated neonatal cardiomyocytes from this strain after *in utero* DE exposure to assess whether cardiomyocytes from exposed animals were more susceptible to hydrogen peroxide-induced apoptosis but did not observe increased susceptibility (unpublished data). Furthermore, we overexpressed both *miR133a* and *PTPRF* in H9c2 myoblasts by lentiviral transduction to assess whether stable changes in the expression of these genes affected the susceptibility of these cells to hydrogen peroxide-induced apoptosis. Unfortunately, in our studies, these cells rapidly undergo necrosis and, thus, an effect of candidate gene overexpression on apoptosis could not be measured (data not shown). Future studies on genetically modified mice that were generated on a C57BL/6 background are needed to truly assess the contribution of these genes to DE-induced susceptibility to heart failure, but are beyond the scope of the current study.

CONCLUSIONS

We have reported significant transcriptional and DNA methylation changes associated with *in utero* DE exposure and adult TAC surgery. Additional analysis of how these genes impact adult susceptibility to heart failure is in progress. Both gain- and loss-of-function models will be informative for the development of air pollution-associated heart failure treatments. *miR133a* has already been identified as a biomarker of patient outcome after valve replacement (57) and is currently being studied as a treatment postinfarction to improve patient outcomes (58). Determining whether *miR133a* can play a similarly protective role in our model of DE-induced heart failure—alongside the potential benefits of decreasing *Ptprf* and *Panr1* expression—will pave the way for further drug development for patients with air pollution-associated heart failure. FJ

ACKNOWLEDGMENTS

The authors thank James Stewart (University of Washington) for expert technical assistance with diesel exhaust exposures. J.M.G. was supported by U.S. National Institutes of Health (NIH) National Institute of Environmental Health Sciences (NIEHS) Training Grant T32 ES007032. C.S.W. was supported by NIH National Heart, Lung, and Blood Institute Training Grant T32 HL007312. J.W.M. and T.K.B. were supported by NIH NIEHS Grant P30ES07033 to the University of

Washington Center for Exposures, Diseases, Genomics and Environment (EDGE). M.T.C. was supported by NIH NIEHS Grant ES023015 and American Heart Association Grant 15GRNT25390012.

AUTHOR CONTRIBUTIONS

J. M. Goodson contributed to hypotheses generation and experimental design, conducted primary cell harvests, prepared samples for bisulfite sequencing, interpreted data, and is the primary author of the manuscript; C. S. Weldy prepared RNA, performed quantitative RT-PCR and echocardiography, interpreted data, and contributed to the preparation of the manuscript; J. W. MacDonald performed key bioinformatics analyses for RNA sequencing and targeted bisulfite sequencing and contributed to the preparation of the manuscript; Y. Liu performed animal surgeries; T. K. Bammler contributed to bioinformatics analyses and to the preparation of the manuscript; W.-M. Chien assisted in molecular biology experiments and contributed to the preparation of the manuscript; M. T. Chin contributed to hypotheses generation and experimental design, contributed to the preparation of the manuscript, and was responsible for overall coordination of the project; and all authors read and approved of the final copy of the manuscript.

REFERENCES

1. Pope III, C. A., Burnett, R. T., Thun, M. J., Calle, E. E., Krewski, D., Ito, K., and Thurston, G. D. (2002) Lung cancer, cardiopulmonary mortality, and long-term exposure to fine particulate air pollution. *JAMA* **287**, 1132–1141
2. Ni, L., Chuang, C. C., and Zuo, L. (2015) Fine particulate matter in acute exacerbation of COPD. *Front. Physiol.* **6**, 294
3. Brook, R. D., Rajagopalan, S., Pope III, C. A., Brook, J. R., Bhatnagar, A., Diez-Roux, A. V., Holguin, F., Hong, Y., Luepker, R. V., Mittleman, M. A., Peters, A., Siscovick, D., Smith, S. C., Jr., Whitsett, L., and Kaufman, J. D.; American Heart Association Council on Epidemiology and Prevention, Council on the Kidney in Cardiovascular Disease, and Council on Nutrition, Physical Activity and Metabolism. (2010) Particulate matter air pollution and cardiovascular disease: an update to the scientific statement from the American Heart Association. *Circulation* **121**, 2331–2378
4. Krishnan, R. M., Adar, S. D., Szpiro, A. A., Jorgensen, N. W., Van Hee, V. C., Barr, R. G., O'Neill, M. S., Herrington, D. M., Polak, J. F., and Kaufman, J. D. (2012) Vascular responses to long- and short-term exposure to fine particulate matter: MESA air (multi-ethnic study of atherosclerosis and air pollution). *J. Am. Coll. Cardiol.* **60**, 2158–2166
5. Pope III, C. A., Muhlestein, J. B., May, H. T., Renlund, D. G., Anderson, J. L., and Horne, B. D. (2006) Ischemic heart disease events triggered by short-term exposure to fine particulate air pollution. *Circulation* **114**, 2443–2448
6. Wang, Y., Eliot, M. N., and Wellenius, G. A. (2014) Short-term changes in ambient particulate matter and risk of stroke: a systematic review and meta-analysis. *J. Am. Heart Assoc.* **3**, e000983
7. Van den Hooven, E. H., Pierik, F. H., de Kluizenaar, Y., Willemsen, S. P., Hofman, A., van Ratingen, S. W., Zandveld, P. Y., Mackenbach, J. P., Steegers, E. A., Miedema, H. M., and Jaddoe, V. W. (2012) Air pollution exposure during pregnancy, ultrasound measures of fetal growth, and adverse birth outcomes: a prospective cohort study. *Environ. Health Perspect.* **120**, 150–156
8. Saenen, N. D., Vrijens, K., Janssen, B. G., Madhloum, N., Peusens, M., Gyselaers, W., Vanpoucke, C., Lefebvre, W., Roels, H. A., and Nawrot, T. S. (2016) Placental nitrosative stress and exposure to ambient air pollution during gestation: a population study. *Am. J. Epidemiol.* **184**, 442–449
9. Barker, D. J., Osmond, C., Golding, J., Kuh, D., and Wadsworth, M. E. (1989) Growth *in utero*, blood pressure in childhood and adult life, and mortality from cardiovascular disease. *BMJ* **298**, 564–567

10. Van Rossem, L., Rifas-Shiman, S. L., Melly, S. J., Kloog, I., Luttmann-Gibson, H., Zanobetti, A., Coull, B. A., Schwartz, J. D., Mittleman, M. A., Oken, E., Gillman, M. W., Koutrakis, P., and Gold, D. R. (2015) Prenatal air pollution exposure and newborn blood pressure. *Environ. Health Perspect.* **123**, 353–359
11. Weldy, C. S., Liu, Y., Chang, Y. C., Medvedev, I. O., Fox, J. R., Larson, T. V., Chien, W. M., and Chin, M. T. (2013) *In utero* and early life exposure to diesel exhaust air pollution increases adult susceptibility to heart failure in mice. *Part. Fibre Toxicol.* **10**, 59
12. Weldy, C. S., Liu, Y., Liggitt, H. D., and Chin, M. T. (2014) *In utero* exposure to diesel exhaust air pollution promotes adverse intrauterine conditions, resulting in weight gain, altered blood pressure, and increased susceptibility to heart failure in adult mice. *PLoS One* **9**, e88582
13. Tarantini, L., Bonzini, M., Apostoli, P., Pegoraro, V., Bollati, V., Marinelli, B., Cantone, L., Rizzo, G., Hou, L., Schwartz, J., Bertazzi, P. A., and Baccarelli, A. (2009) Effects of particulate matter on genomic DNA methylation content and iNOS promoter methylation. *Environ. Health Perspect.* **117**, 217–222
14. Baccarelli, A., Wright, R. O., Bollati, V., Tarantini, L., Litonjua, A. A., Suh, H. H., Zanobetti, A., Sparrow, D., Vokonas, P. S., and Schwartz, J. (2009) Rapid DNA methylation changes after exposure to traffic particles. *Am. J. Respir. Crit. Care Med.* **179**, 572–578
15. Janssen, B. G., Godderis, L., Pieters, N., Poels, K., Kiciński, M., Cuyper, A., Fierens, F., Penders, J., Plusquin, M., Gyselaers, W., and Nawrot, T. S. (2013) Placental DNA hypomethylation in association with particulate air pollution in early life. *Part. Fibre Toxicol.* **10**, 22
16. Weldy, C. S., Luttrell, I. P., White, C. C., Morgan-Stevenson, V., Cox, D. P., Carosino, C. M., Larson, T. V., Stewart, J. A., Kaufman, J. D., Kim, F., Chitale, K., and Kavanagh, T. J. (2013) Glutathione (GSH) and the GSH synthesis gene *Gclm* modulate plasma redox and vascular responses to acute diesel exhaust inhalation in mice. *Inhal. Toxicol.* **25**, 444–454
17. Gould, T., Larson, T., Stewart, J., Kaufman, J. D., Slater, D., and McEwen, N. (2008) A controlled inhalation diesel exhaust exposure facility with dynamic feedback control of PM concentration. *Inhal. Toxicol.* **20**, 49–52
18. Yin, F., Lawal, A., Ricks, J., Fox, J. R., Larson, T., Navab, M., Fogelman, A. M., Rosenfeld, M. E., and Araujo, J. A. (2013) Diesel exhaust induces systemic lipid peroxidation and development of dysfunctional pro-oxidant and pro-inflammatory high-density lipoprotein. *Arterioscler. Thromb. Vasc. Biol.* **33**, 1153–1161
19. Liu, Y., Chien, W. M., Medvedev, I. O., Weldy, C. S., Luchtel, D. L., Rosenfeld, M. E., and Chin, M. T. (2013) Inhalation of diesel exhaust does not exacerbate cardiac hypertrophy or heart failure in two mouse models of cardiac hypertrophy. *Part. Fibre Toxicol.* **10**, 49
20. Liao, Y., Smyth, G. K., and Shi, W. (2013) The subread aligner: fast, accurate and scalable read mapping by seed-and-vote. *Nucleic Acids Res.* **41**, e108
21. Greco, S., Fasanaro, P., Castelvécchio, S., D'Alessandra, Y., Arcelli, D., Di Donato, M., Malavazos, A., Capogrossi, M. C., Menicanti, L., and Martelli, F. (2012) MicroRNA dysregulation in diabetic ischemic heart failure patients. *Diabetes* **61**, 1633–1641
22. Liu, Y., Yu, M., Wu, L., and Chin, M. T. (2010) The bHLH transcription factor CHF1/Hey2 regulates susceptibility to apoptosis and heart failure after pressure overload. *Am. J. Physiol. Heart Circ. Physiol.* **298**, H2082–H2092
23. Xiang, F., Sakata, Y., Cui, L., Youngblood, J. M., Nakagami, H., Liao, J. K., Liao, R., and Chin, M. T. (2006) Transcription factor CHF1/Hey2 suppresses cardiac hypertrophy through an inhibitory interaction with GATA4. *Am. J. Physiol. Heart Circ. Physiol.* **290**, H1997–H2006
24. Bolger, A. M., Lohse, M., and Usadel, B. (2014) Trimmomatic: a flexible trimmer for Illumina sequence data. *Bioinformatics* **30**, 2114–2120
25. Krueger, F., and Andrews, S. R. (2011) Bismark: a flexible aligner and methylation caller for Bisulfite-Seq applications. *Bioinformatics* **27**, 1571–1572
26. Langmead, B., Trapnell, C., Pop, M., and Salzberg, S. L. (2009) Ultrafast and memory-efficient alignment of short DNA sequences to the human genome. *Genome Biol.* **10**, R25
27. Hansen, K. D., Langmead, B., and Irizarry, R. A. (2012) BSmooth: from whole genome bisulfite sequencing reads to differentially methylated regions. *Genome Biol.* **13**, R83
28. Feng, H., Conneely, K. N., and Wu, H. (2014) A bayesian hierarchical model to detect differentially methylated loci from single nucleotide resolution sequencing data. *Nucleic Acids Res.* **42**, e69
29. Carè, A., Catalucci, D., Felicetti, F., Bonci, D., Addario, A., Gallo, P., Bang, M. L., Segnalini, P., Gu, Y., Dalton, N. D., Elia, L., Latronico, M. V., Høydal, M., Autore, C., Russo, M. A., Dorn II, G. W., Ellingsen, O., Ruiz-Lozano, P., Peterson, K. L., Croce, C. M., Peschle, C., and Condorelli, G. (2007) MicroRNA-133 controls cardiac hypertrophy. *Nat. Med.* **13**, 613–618
30. Condorelli, G., Diwan, A., Nerbonne, J. M., and Dorn II, G. W. (2010) MicroRNA-133a protects against myocardial fibrosis and modulates electrical repolarization without affecting hypertrophy in pressure-overloaded adult hearts. *Circ. Res.* **106**, 166–175
31. Brauer, M., Freedman, G., Frostad, J., van Donkelaar, A., Martin, R. V., Dentener, F., van Dingenen, R., Estep, K., Amini, H., Apté, J. S., Balakrishnan, K., Barregard, L., Broday, D., Feigin, V., Ghosh, S., Halokh, P. K., Knibbs, L. D., Kokubo, Y., Liu, Y., Ma, S., Morawska, L., Sangrador, J. L., Shaddick, G., Anderson, H. R., Vos, T., Forouzanfar, M. H., Burnett, R. T., and Cohen, A. (2016) Ambient air pollution exposure estimation for the Global Burden of Disease 2013. *Environ. Sci. Technol.* **50**, 79–88
32. Lewné, M., Plato, N., and Gustavsson, P. (2007) Exposure to particles, elemental carbon and nitrogen dioxide in workers exposed to motor exhaust. *Ann. Occup. Hyg.* **51**, 693–701
33. Nakayama, Y., Nara, N., Kawakita, Y., Takeshima, Y., Arakawa, M., Katoh, M., Morita, S., Iwatsuki, K., Tanaka, K., Okamoto, S., Kitamura, T., Seki, N., Matsuda, R., Matsuo, M., Saito, K., and Hara, T. (2004) Cloning of cDNA encoding a regeneration-associated muscle protease whose expression is attenuated in cell lines derived from Duchenne muscular dystrophy patients. *Am. J. Pathol.* **164**, 1773–1782
34. Sharma, P. R., Mackey, A. J., Dejene, E. A., Ramadan, J. W., Langefeld, C. D., Palmer, N. D., Taylor, K. D., Wagenknecht, L. E., Watanabe, R. M., Rich, S. S., and Nunemaker, C. S. (2015) An islet-targeted genome-wide association scan identifies novel genes implicated in cytokine-mediated islet stress in type 2 diabetes. *Endocrinology* **156**, 3147–3156
35. Lo, P. H., Tanikawa, C., Katagiri, T., Nakamura, Y., and Matsuda, K. (2015) Identification of novel epigenetically inactivated gene PAMRI in breast carcinoma. *Oncol. Rep.* **33**, 267–273
36. Tonks, N. K. (2013) Protein tyrosine phosphatases—from housekeeping enzymes to master regulators of signal transduction. *FEBS J.* **280**, 346–378
37. Chagnon, M. J., Uetani, N., and Tremblay, M. L. (2004) Functional significance of the LAR receptor protein tyrosine phosphatase family in development and diseases. *Biochem. Cell Biol.* **82**, 664–675
38. Zhang, W. R., Li, P. M., Oswald, M. A., and Goldstein, B. J. (1996) Modulation of insulin signal transduction by eutopic overexpression of the receptor-type protein-tyrosine phosphatase LAR. *Mol. Endocrinol.* **10**, 575–584
39. Zabolotny, J. M., Kim, Y. B., Peroni, O. D., Kim, J. K., Pani, M. A., Boss, O., Klamann, L. D., Kamatkar, S., Shulman, G. I., Kahn, B. B., and Neel, B. G. (2001) Overexpression of the LAR (leukocyte antigen-related) protein-tyrosine phosphatase in muscle causes insulin resistance. *Proc. Natl. Acad. Sci. USA* **98**, 5187–5192
40. Kulas, D. T., Zhang, W. R., Goldstein, B. J., Furlanetto, R. W., and Mooney, R. A. (1995) Insulin receptor signaling is augmented by antisense inhibition of the protein tyrosine phosphatase LAR. *J. Biol. Chem.* **270**, 2435–2438
41. Menzaghi, C., Paroni, G., De Bonis, C., Coco, A., Vigna, C., Miscio, G., Lanna, P., Tassi, V., Bacci, S., and Trischitta, V. (2008) The protein tyrosine phosphatase receptor type f (PTPRF) locus is associated with coronary artery disease in type 2 diabetes. *J. Intern. Med.* **263**, 653–654
42. Ahmad, F., and Goldstein, B. J. (1997) Functional association between the insulin receptor and the transmembrane protein-tyrosine phosphatase LAR in intact cells. *J. Biol. Chem.* **272**, 448–457
43. Liu, N., Bezprozvannaya, S., Williams, A. H., Qi, X., Richardson, J. A., Bassel-Duby, R., and Olson, E. N. (2008) microRNA-133a regulates cardiomyocyte proliferation and suppresses smooth muscle gene expression in the heart. *Genes Dev.* **22**, 3242–3254
44. Drawnel, F. M., Wachten, D., Molkenin, J. D., Maillet, M., Aronsen, J. M., Swift, F., Sjaastad, I., Liu, N., Catalucci, D., Mikoshiba, K., Hisatsune, C., Okkenhaug, H., Andrews, S. R., Bootman, M. D., and Roderick, H. L. (2012) Mutual antagonism between IP(3)RII and miRNA-133a regulates calcium signals and cardiac hypertrophy. *J. Cell Biol.* **199**, 783–798
45. He, B., Xiao, J., Ren, A. J., Zhang, Y. F., Zhang, H., Chen, M., Xie, B., Gao, X. G., and Wang, Y. W. (2011) Role of miR-1 and miR-133a in myocardial ischemic postconditioning. *J. Biomed. Sci.* **18**, 22

46. Liu, N., Bezprozvannaya, S., Shelton, J. M., Frisard, M. I., Hulver, M. W., McMillan, R. P., Wu, Y., Voelker, K. A., Grange, R. W., Richardson, J. A., Bassel-Duby, R., and Olson, E. N. (2011) Mice lacking microRNA 133a develop dynamin 2-dependent centronuclear myopathy. *J. Clin. Invest.* **121**, 3258–3268
47. Chen, W. S., Leung, C. M., Pan, H. W., Hu, L. Y., Li, S. C., Ho, M. R., and Tsai, K. W. (2012) Silencing of miR-1-1 and miR-133a-2 cluster expression by DNA hypermethylation in colorectal cancer. *Oncol. Rep.* **28**, 1069–1076
48. Huang, L., Xi, Z., Wang, C., Zhang, Y., Yang, Z., Zhang, S., Chen, Y., and Zuo, Z. (2016) Phenanthrene exposure induces cardiac hypertrophy via reducing miR-133a expression by DNA methylation. *Sci. Rep.* **6**, 20105
49. Westerholm, R., Christensen, A., Törnqvist, M., Ehrenberg, L., Rannug, U., Sjögren, M., Raftar, J., Soontjens, C., Almén, J., and Gränn, K. (2001) Comparison of exhaust emissions from Swedish Environmental classified diesel fuel (MK1) and European Program on Emissions, Fuels and Engine Technologies (EPEFE) reference fuel: a chemical and biological characterization, with viewpoints on cancer risk. *Environ. Sci. Technol.* **35**, 1748–1754
50. Gilsbach, R., Preissl, S., Grüning, B. A., Schnick, T., Burger, L., Benes, V., Würch, A., Bönisch, U., Günther, S., Backofen, R., Fleischmann, B. K., Schübeler, D., and Hein, L. (2014) Dynamic DNA methylation orchestrates cardiomyocyte development, maturation and disease. *Nat. Commun.* **5**, 5288
51. Wauters, A., Dreyfuss, C., Pochet, S., Hendrick, P., Berkenboom, G., van de Borne, P., and Argacha, J. F. (2013) Acute exposure to diesel exhaust impairs nitric oxide-mediated endothelial vasomotor function by increasing endothelial oxidative stress. *Hypertension* **62**, 352–358
52. Zuo, L., Youtz, D. J., and Wold, L. E. (2011) Particulate matter exposure exacerbates high glucose-induced cardiomyocyte dysfunction through ROS generation. *PLoS One* **6**, e23116
53. Valinluck, V., Tsai, H. H., Rogstad, D. K., Burdzy, A., Bird, A., and Sowers, L. C. (2004) Oxidative damage to methyl-CpG sequences inhibits the binding of the methyl-CpG binding domain (MBD) of methyl-CpG binding protein 2 (MeCP2). *Nucleic Acids Res.* **32**, 4100–4108
54. Hackett, J. A., Sengupta, R., Zylicz, J. J., Murakami, K., Lee, C., Down, T. A., and Surani, M. A. (2013) Germline DNA demethylation dynamics and imprint erasure through 5-hydroxymethylcytosine. *Science* **339**, 448–452
55. Guo, J. U., Su, Y., Zhong, C., Ming, G. L., and Song, H. (2011) Hydroxylation of 5-methylcytosine by TET1 promotes active DNA demethylation in the adult brain. *Cell* **145**, 423–434
56. Brenet, F., Moh, M., Funk, P., Feierstein, E., Viale, A. J., Socci, N. D., and Scandura, J. M. (2011) DNA methylation of the first exon is tightly linked to transcriptional silencing. *PLoS One* **6**, e14524
57. García, R., Villar, A. V., Cobo, M., Llano, M., Martín-Durán, R., Hurlé, M. A., and Nistal, J. F. (2013) Circulating levels of miR-133a predict the regression potential of left ventricular hypertrophy after valve replacement surgery in patients with aortic stenosis. *J. Am. Heart Assoc.* **2**, e000211
58. Dakhllallah, D., Zhang, J., Yu, L., Marsh, C. B., Angelos, M. G., and Khan, M. (2015) MicroRNA-133a engineered mesenchymal stem cells augment cardiac function and cell survival in the infarct heart. *J. Cardiovasc. Pharmacol.* **65**, 241–251

Received for publication January 11, 2017.

Accepted for publication July 10, 2017.